Journal of Operation and Automation in Power Engineering

Vol. 14, No. 4, Dec. 2026, Pages: 297-307

http://joape.uma.ac.ir

Research Paper

Improving Power Quality in a Microgrid through Control of Active and Reactive Power Output from Inverter-Based Sources

Moein Ganjian and *Ali Ghasemi-Marzbali* *

Department of Electrical and Biomedical Engineering, Mazandaran University of Science and Technology, Babol, Iran.

Abstract— *The increasing integration of inverter-based sources in microgrids demands advanced control strategies to maintain power quality by mitigating harmonics and distortion. This study proposes an enhanced control system for grid-connected inverters, integrating a proportional-integral (PI) controller in the synchronous rotating frame with a repetitive control (RC) compensator. A particle swarm optimization (PSO) algorithm is employed to optimize the controller parameters, ensuring effective harmonic suppression. The proposed PI+RC controller is evaluated through simulation studies under various scenarios, including linear and nonlinear loads as well as grid voltage distortion. Results demonstrate a significant reduction in total harmonic distortion (THD), with the proposed controller achieving a reduction from 37.5% to 5.6% under nonlinear load conditions and from 49.5% to 5% when both nonlinear loads and voltage distortion are present. Additionally, the proposed method effectively stabilizes the active and reactive power outputs, surpassing conventional PI controllers.*

Keywords—Inverter, grid-connected, particle optimization algorithm, power quality, proportional-integral current controller, repetitive controller.

1. Introduction

1.1. Background and motivation

The increasing deployment of distributed generation (DG) units and renewable energy sources has led to a paradigm shift in modern power systems, driving demand for microgrids [1]. These microgrids integrate inverter-based energy resources, enabling decentralized energy management and enhancing grid resilience [2]. However, power quality issues remain a critical challenge due to the nonlinear characteristics of certain loads and the presence of voltage distortions in the grid. The proliferation of nonlinear loads, such as power electronic converters, introduces harmonic distortions that degrade the quality of electrical power, affecting both system stability and operational efficiency [3]. Traditionally, proportional-integral (PI) controllers have been widely adopted for inverter current control in grid-connected applications. While effective under ideal conditions, their performance significantly deteriorates in the presence of harmonics and grid voltage distortions. The need for an advanced control strategy that can mitigate harmonic distortion while ensuring stable power injection is increasingly evident [4]. Various solutions, including proportional-resonant controllers and model predictive control techniques, have been proposed, yet they often suffer from implementation complexity, high computational demands, and sensitivity to system parameter variations [5]. Motivated by these challenges, this study proposes an optimized control system for grid-connected inverters that combines a PI controller with a repetitive control (RC) compensator. The integration of an RC-based compensator enhances harmonic attenuation, ensuring compliance with power quality standards. Additionally, a particle swarm optimization (PSO) algorithm is employed to optimize controller parameters, further improving performance.

1.2. Literature review

Several research studies have been conducted in this field, addressing various control strategies and challenges, which are reviewed in the following section. In [6], a novel capacitor-based multi-level inverter topology is introduced, integrating two cross-square-switched T-Type inverters. This structure supports both modular and cascaded configurations, with the cascaded mode enabling higher voltage levels using low-power switches. In [7], a hybrid switched-capacitor inverter is proposed to minimize component count and ensure automatic capacitor balancing. The design merges a switched capacitor (SC) unit with a flying capacitor (FC). Key benefits include fewer components, simplified control, voltage boosting, and lower inrush current during capacitor charging. In [8], a novel method is proposed for harmonics compensation in grid-connected microgrids (MGs). If sensitive loads are present at the point of common coupling (PCC), voltage harmonics are reduced; otherwise, current harmonics are mitigated to limit grid-side distortion. In both cases, the interface converters of distributed generation (DG) units perform the compensation. A new virtual impedance structure is also introduced to reduce phase impedance asymmetry in the MG. In [9], stability challenges in islanded microgrids—disconnected from the main grid at the point of common coupling (PCC) are addressed. These microgrids, powered by renewable sources such as PV systems, wind turbines, and energy storage, rely on inverters to emulate synchronous generators. To manage voltage and frequency stability, droop control is employed to regulate the active and reactive power

Received: 22 Sept. 2024
Revised: 09 Jun. 2025
Accepted: 10 Jun. 2025
*Corresponding author:
E-mail: ali.ghasemi@ustmb.ac.ir (A. Ghasemi-Marzbali)
DOI: 10.22098/joape.2025.15894.2223

of distributed generators (DGs). In [10], a robust and efficient control strategy is presented for islanded microgrids (MGs) using a master-slave (MS) configuration. The proposed terminal sliding mode control offers fast dynamic response, strong convergence, and resilience to parameter uncertainties. It ensures high stability and performance, enabling inverter-based distributed generation (DG) units to maintain low harmonic distortion in output voltage while accurately tracking active and reactive power references. In [11], the stability of autonomous microgrids is analyzed, considering the low inertia of inverter-based distributed generation (DG) units. The fast inverter dynamics and variability of renewable sources can lead to uneven load sharing during sudden load changes, significantly impacting system stability. The study evaluates microgrid behavior under passive, active, and dynamic loads using small-signal analysis, highlighting the influence of inverter and load parameters. Participation analysis is also used to identify the dominant system states contributing to oscillatory modes.

In [12], hybrid energy storage systems combining batteries and supercapacitors are optimized for better energy management in power networks. These systems address challenges like power quality and voltage stabilization, but effective control remains a key issue. The study reviews conventional control methods and their limitations, proposing a novel approach that integrates fuzzy logic and rule-based systems to address these challenges. In [13], a model and control strategy for a six-switch VSI connected to an AC microgrid is presented, controlling active and reactive power in the dq reference frame. A state feedback control strategy with disturbance cancellation is proposed, using either a voltage sensor or an extended high-gain observer (EHGO) for disturbance estimation. The EHGO-based approach removes the need for a voltage sensor. In [14], a reactive and active power controller is applied to a three-phase grid-connected PV system to enhance power quality using the Seagull Optimization Algorithm (SOA). The system features two main controllers: a Flyback converter optimized with the Bacterial Foraging Optimization Algorithm (BFOA) to maximize PV power and an SOA-based controller for the grid-connected inverter. In [15], the increasing integration of solar photovoltaic energy into the grid is discussed, emphasizing its advantages such as clean energy, easy installation, and improved grid synchronization. A single-stage system is preferred to reduce costs, and while DC-to-DC converters track maximum power, proper inverter control can eliminate their necessity. In [16], a new smart grid application for power system operation is proposed. A Static Compensator (STATCOM) is used to enhance power quality, improve power flow, reduce harmonics, and compensate for reactive power. The STATCOM is based on a quasi-Z-Source Inverter (qZSI) and connected to a Three-Phase Four-Wire (3P4W) distribution system. In [17], renewable energy sources (RESs) and energy storage systems (ESSs) in microgrids (MGs) are explored for stable power supply. Bidirectional power converters (BPCs) manage power flow but face stability and power quality challenges. To address these, a voltage-oriented control (VOC) strategy is developed for an LCL-filtered grid-connected bidirectional AC–DC converter, incorporating an inner current control loop (ICCL) and active damping to estimate capacitor current. In [18], the power sector's shift toward decentralized generation is explored, with microgrids integrating renewable and traditional energy sources. To enhance reliability and power quality (PQ), a hybrid model combining photovoltaics, wind energy, and fuel cells is proposed, integrated with a UPQC to address PQ challenges. The system utilizes a Back-stepping controller with Model Reference Adaptive Control (MRAC) and online parameter tuning, providing improved adaptability, efficiency, and stability for optimal grid management. In [19], a modified power control (MPC) strategy is proposed for a grid-connected autonomous microgrid with multiple solar photovoltaic inverter (SPI) units. The MPC enables seamless switching between grid-tied mode (GTM) and islanding mode (IAM). In GTM, SPIs supply power to the load while feeding excess power to the grid at unity power factor. During a grid failure, the main SPI switches from current control mode (CCM) in GTM to voltage control mode (VCM) in IAM, ensuring uninterrupted power supply to the load. For reader convenience, in [20], the decline of traditional energy sources and growing demand highlight the need for renewable alternatives. Distributed Generation (DG) from renewables, especially MicroGrids (MGs), offers a viable solution but introduces power quality (PQ) issues such as harmonic generation and reactive power compensation. These issues, caused by converters and switching devices, are amplified by renewable intermittency and nonlinear loads. The paper reviews methods to improve PQ in MGs, including filters, controllers, FACTS devices, optimization techniques, and machine learning, based on a survey of 350 recent articles.

1.3. Literature gap and paper contribution

The increasing integration of inverter-based sources into microgrids has brought about significant challenges related to power quality, primarily due to nonlinear loads and grid voltage distortions. While various control strategies have been proposed to address these issues—such as proportional-resonant controllers and model predictive control—they often suffer from complex implementations, high computational demands, and sensitivity to parameter variations. Conventional proportional-integral (PI) controllers, widely used for inverter current control, also face notable performance degradation under distorted grid conditions, failing to adequately suppress harmonics. This study addresses these gaps by proposing an optimized control system that combines a PI controller with a repetitive control (RC) compensator. The integration of the RC compensator enhances harmonic filtering capability, enabling the system to meet power quality standards while maintaining computational efficiency. Furthermore, while previous research has focused on improving the design of controllers, there has been little emphasis on systematically optimizing controller parameters to ensure maximum performance. In this study, a Particle Swarm Optimization (PSO) algorithm is employed to fine-tune the parameters of the PI+RC controller, ensuring optimal harmonic suppression and stabilization of active and reactive power outputs. This approach significantly enhances the controller's ability to handle various grid conditions, including nonlinear loads and voltage distortions, and outperforms conventional PI controllers. The main contributions and novelties of this paper can be summarized as follows:

- Proposes a combination of a proportional-integral (PI) controller with a repetitive control (RC) compensator to enhance harmonic suppression and power quality.
- Employs Particle Swarm Optimization (PSO) to fine-tune controller parameters for optimal performance under varying grid conditions.
- Demonstrates a remarkable reduction in total harmonic distortion (THD) from 37.5% to 5.6% in nonlinear load conditions, and from 49.5% to 5% with both nonlinear loads and voltage distortion.
- The proposed PI+RC controller achieves superior performance in harmonic suppression and power stability compared to traditional PI controllers.

2. Problem Modeling

2.1. Proportional-integral controller

In this section, a proportional-integral (PI) controller is first considered for a grid-connected inverter equipped with an inductive-capacitive (LC) filter. The objective of this setup is to gain familiarity with the operation of the current control system and to understand its requirements and response characteristics. The PI controller is widely adopted in industry across various applications due to its effective performance, simple structure, and ease of implementation. Accordingly, this research also adopts a PI-based controller as its foundation. A current controller based

on the PI approach is therefore designed and implemented for the specified inverter. The primary goal of the PI current controller is to generate an appropriate reference signal for the inverter, enabling it to deliver a defined amount of active and reactive power at its output, as specified by the reference power. As a result, it is necessary to calculate and control the active and reactive power outputs of the inverter independently. Considering the control strategies discussed in the previous section, implementing the controller within a synchronous rotating reference frame is a highly suitable approach for achieving this objective. Since the signals are transformed into DC quantities in $abc \rightarrow dq0$ frame, they are highly compatible with PI control.

Fig. 1 illustrates the structure of a power network where an inverter converts a steady DC source voltage into AC voltage. The LC filter significantly reduces the voltage distortion introduced by the inverter, resulting in an output voltage across the capacitor that is nearly sinusoidal.

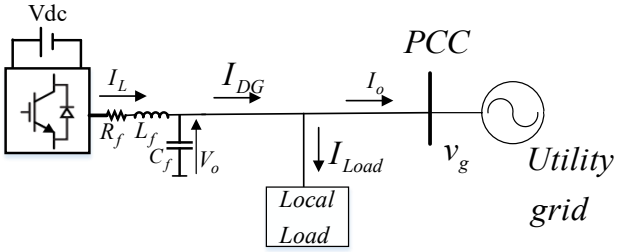

Fig. 1. Shows the structure of the power system under study.

For the above network, active and reactive powers are calculated as follows:

$$P_o = \frac{3}{2}(V_{gd}I_{od} + V_{gq}I_{oq}) \tag{1}$$

$$Q_o = \frac{3}{2}(-V_{gd}I_{oq} + V_{gq}I_{od}) \tag{2}$$

Where V_{gd} and V_{gq} are the direct and quadrature components of the network voltage at the Point of Common Coupling (PCC), and I_{od} and I_{oq} are the direct and quadrature components of the input current to the power network. In fact, this current is calculated as the difference between the current produced by the inverter and the current drawn by the load. However, in real-world applications, this current is typically measured using a current sensor or a current transformer. For the above grid-connected inverter, a proportional-integral (PI) current controller will be designed and implemented to regulate the output and deliver the specified amount of active and reactive power.

2.2. Implementation of the proportional-integral controller

For the design of the proportional-integral (PI) controller, the configuration shown in Fig. 2 is used. The output current I_o serves as the input to the current controller. Fig. 2 illustrates the implementation of the PI controller used for regulating the inverter current in a grid-connected configuration.

Initially, the reference currents for the direct (d) and quadrature (q) components are calculated using the corresponding equations based on the desired active and reactive power inputs. In the next step, the difference between the measured current transformed into the dq reference frame and the calculated reference currents is determined. These differences serve as error signals and are fed into the proportional-integral (PI) controller. The output of the PI controller is then added to the direct and quadrature components of the network voltage, resulting in the generation of the voltage reference signal in the dq domain. To apply this reference signal

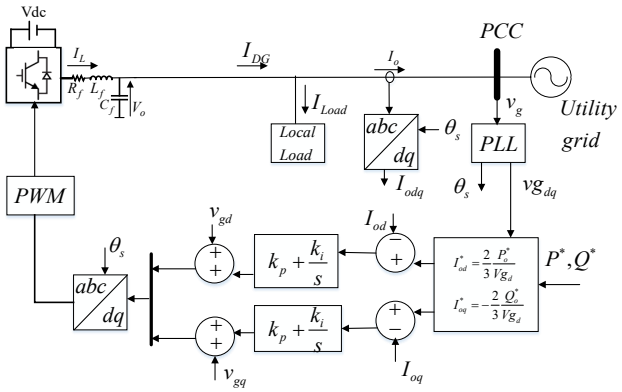

Fig. 2. Connection structure of a distributed generator to the grid at the PCC along with the current controller based on the proportional-integral controller [21].

to the pulse-width modulation (PWM) unit and subsequently to the inverter, it must be transformed from the dq domain back to the three-phase (abc) domain. This transformation is performed by the inverse Park transformation block.

It is important to note that the controller is designed in the synchronous rotating dq reference frame. Therefore, all three-phase signals including current and voltage used by the controller must be transformed into DC components using the Park transformation matrix. All signals first pass through the dq domain, and after processing by the controllers, they must be converted back to the three-phase domain. The implementation requires the use of the following transformation matrix:

$$\begin{bmatrix} d \\ q \\ 0 \end{bmatrix} = \frac{2}{3}\begin{bmatrix} \cos\theta_s & \cos(\theta_s - 2\pi/3) & \cos(\theta_s + 2\pi/3) \\ -\sin\theta_s & -\sin(\theta_s - 2\pi/3) & -\sin(\theta_s + 2\pi/3) \\ \frac{1}{2} & \frac{1}{2} & \frac{1}{2} \end{bmatrix}\begin{bmatrix} a \\ b \\ c \end{bmatrix} \tag{3}$$

Where θ_s is the voltage phase that rotates at synchronous speed (grid frequency). It is clear that for converting the three-phase domain to the direct and quadrature components dq or vice versa, it is necessary to have the voltage phase at each moment in time [22].

2.3. Challenges of proportional-integral control

For the network under study, it was initially assumed that the local load at the inverter output exhibits linear behavior. Impedance loads, such as resistive and resistive-inductive types, typically behave linearly. Examples of such loads include incandescent lamps and electric heaters. However, today, the presence of such linear loads in low-voltage networks is not prevalent, and with the increasing proliferation of high-power electronic devices, the number of nonlinear loads is rapidly growing. One significant effect of nonlinear loads is the generation of distortion and harmonics in the current, which can easily propagate into the network. Harmonics can cause interference in protective and communication control systems, damage transformers, motors, and conductors, and increase currents in capacitors. In power transformers and rotating machines, harmonics cause a reduction in the power factor ($\cos\ \Phi$), premature aging of insulation materials leading to loss of dielectric properties, increased heat generation, and higher operating temperatures especially in transformers and cables—thereby reducing the lifespan of these devices.

Harmonics, which distort the voltage waveform, are present in nonlinear loads such as motors and create circulating currents

in conductors exposed to varying magnetic fields, which in turn reduces torque. In unbalanced systems, harmonics can cause the neutral current to exceed the sum of the phase currents at the fundamental frequency, potentially overloading the neutral conductor. Mechanical vibrations and rotational oscillations in electric machines may cause asymmetry in the shaft and damage the stator, rotor, and bearings. Besides harmonic generation by nonlinear loads such as rectifiers, power grid voltage distortion can arise due to various factors, significantly increasing the overall Total Harmonic Distortion (THD). Therefore, it is crucial to reduce harmonic distortion to acceptable levels. According to IEEE 1547, the standard value for current THD at low-voltage network levels is approximately 5% [23]. Thus, it is necessary for the proportional-integral (PI) controller to perform optimally in the presence of nonlinear loads or harmonic distortion in general. As mentioned, the PI controller performs well only when its input signals are DC, which is achieved in the dq domain. In the absence of harmonic distortion, a three-phase sinusoidal signal converts into two pure DC signals in the dq domain. However, when harmonic distortion exists, in addition to the fundamental grid frequency, harmonic frequencies (commonly multiples of 5 and 7) are present. Applying the transformation matrix, these harmonic components also appear in the dq domain as DC signals with oscillatory noise. Consequently, the PI controller receives a noisy DC input rather than a clean one, which severely degrades its performance and may even cause instability. In fact, the poor performance of the PI controller not only fails to eliminate harmonic distortion and reduce THD below the standard value but may also increase THD. Therefore, the goal when using the controller with harmonic distortion present is to reduce the current THD and improve the power quality of the electrical network.

In the passive method, passive components such as inductors and capacitors are used. The values of these components can be designed to filter out current or voltage harmonics present in the network. However, as harmonic levels increase, more filters are required, which is not economically feasible. Additionally, because harmonic content varies with different loading conditions, adjustments to the inductors and capacitors are necessary, which is impractical. In the active method, active devices present in the network are utilized. Inverters are recognized as active equipment with very high response speeds and controllability. By measuring current and voltage and determining harmonic content, inverters can switch appropriately to produce specific voltage and current outputs that reduce harmonic distortion to acceptable levels. The prerequisite for this function is an appropriate control system capable of filtering the desired harmonics.

3. Proposed Method

Given the satisfactory performance of the proportional-integral controller, the proposed controller builds upon it. However, to improve the quality of electrical power and reduce the THD injected into the power network, it is necessary to add a supplementary controller. The supplementary controller should operate so that the generated reference signal optimizes the inverter switching to effectively reduce harmonics. Therefore, the proposed supplementary controller is designed specifically to eliminate harmonics. The Repetitive Controller (RC) is one of the controllers with proven satisfactory performance in eliminating harmonics. The structure of the RC controller is shown in Fig. 3.

In this structure, the gain of the RC controller (k_r), a pre-phase block (z^k), a time delay ($z^{-N/6}$), and a low-pass filter ($Q(z)$) in the discrete domain (Z-transform) are included [24]. The structure of this low-pass filter is as follows:

$$Q(z) = a_1 z + a_0 + a_1 z^{-1} \tag{4}$$

where $2a_1 + a_0 = 1$. The transfer function of the aforementioned repetitive controller is obtained as follows:

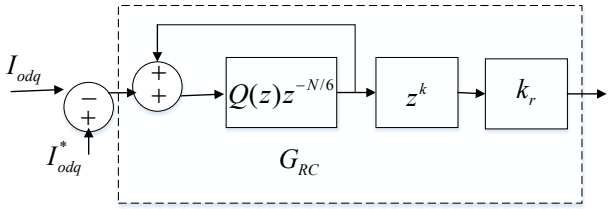

Fig. 3. Structure of the proposed RC controller.

$$G_{RC}(z) = \frac{a_1 z^{k+2} + a_0 z^{k+1} + a_1 z^k}{z^{1+N/6} - a_1 z^2 - a_0 z^1 - a_1} \tag{5}$$

For example, $a_0 = \frac{1}{2}$ and $a_1 = \frac{1}{4}$, the frequency response of the RC controller would appear as shown in Fig. 4.

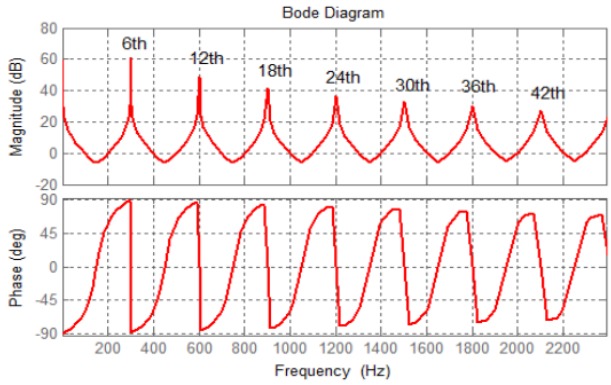

Fig. 4. Frequency response of the RC controller.

As seen in the figure, the controller has high gain at frequencies of the 6th, 12th, 18th, 24th orders, and so on, meaning it acts as a filter for these harmonics, effectively preventing their passage. It is noteworthy that the harmonics in the three-phase domain shift by one order in the dq domain. For instance, the 6th order in the dq domain corresponds to the 5th and 7th orders in the three-phase domain. The time delay $z^{-N/6}$ should be designed to ensure optimal performance. Therefore, the value of N is calculated from the following relation:

$$N = \frac{f_{switching}}{f_s} \tag{6}$$

Where $f_{switching}$ is the switching frequency of the inverter and f_s is the frequency of the power network.

3.1. Implementation of the proposed control structure based on PI+RC

With the implementation of the proposed RC method into the control structure of Fig. 2, the proposed control structure, aimed at injecting specific power and improving the quality of electrical power, appears as Fig. 5. In the proposed structure, the Proportional-Integral (PI) controller is used for tracking the power injected into the grid by the inverter. The PI controller also provides satisfactory stability. In fact, the primary goal in controlling grid-connected inverters, which is the injection of specified power, is achieved by the PI controller. The secondary goal, which is to improve the quality of electrical power and reduce the THD of the output current of the inverter (injected into the power grid), is achieved by the RC controller. It is crucial to note that the correct selection of parameters for the PI and RC

controllers plays a direct role in the performance of the proposed controller. Incorrect values can enhance distortion and increase the THD level.

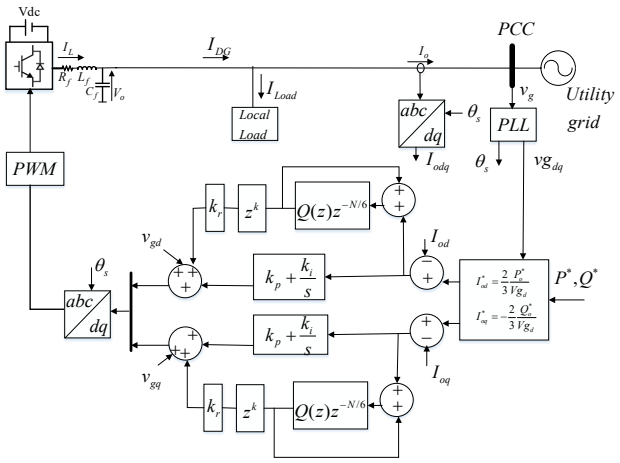

Fig. 5. Proposed PI+RC control structure for a distributed generator connected to the grid at the PCC.

3.2. Design of the proposed controller

After introducing the proposed controller, it is necessary to accurately determine the values of its various parameters. The correct selection of these parameters directly affects overall system performance and the elimination of harmonics. Therefore, the use of optimization algorithms is considered an appropriate solution. The first step in using optimization algorithms is to define and formulate a suitable objective function along with the technical constraints involved in the problem. The objective function in this article is defined as follows:

$$\text{Objective min f} = \sum \left(I_{od} - {I_{od}}^{ref}\right)^2 + \left(I_{oq} - {I_{oq}}^{ref}\right)^2 + \alpha \times \max(\text{THD}) \tag{7}$$

Where in the above equation, I_{od} and I_{oq} are the d and q components of the output current of the inverter, respectively. I_{od}^{ref} and I_{oq}^{ref} are the reference values for the d and q components of the output current of the inverter, and THD is the level of harmonic distortion in the output current of the inverter.

3.3. Particle Swarm Optimization algorithm

Particle Swarm Optimization (PSO) is a search algorithm inspired by the social dynamics observed in bird flocks. Originally, this algorithm was designed to understand how birds fly synchronously, make quick directional changes, and form optimal group patterns. In PSO, individual particles traverse a search space, guided by both their own experiences and the insights gained from neighboring particles. The behavior of nearby clusters of particles influences how each particle explores the space, causing them to gravitate toward promising regions. Through this process, particles share knowledge and adjust their positions, moving toward the most successful areas identified by their peers. The core principle of PSO is that each particle continuously updates its position based on the best outcomes it has individually encountered and the best results found within its neighborhood. The goal of optimization problems is to identify a variable, represented by the vector $X = [x_1, x_2, x_3, \ ..., x_n]$, that either maximizes or minimizes the objective function f(X), depending on its formulation. The vector X, referred to as a position vector, embodies the variable model and is an n-dimensional vector, where n represents the number of variables involved in the problem. For instance, in determining the optimal landing spot for a flock of birds, n would correspond to the geographical coordinates, such as longitude and latitude. This section provides a brief overview of standard PSO, with a comprehensive explanation available in [25]. In PSO, each particle has a unique velocity, which is updated according to specific formulas:

$$v_{i,d}(t+1) = wv_{i,d}(t) + c_1 r_1(p_{best} - x_{i,d}(t)) + c_2 r_2(g_{best} - x_{i,d}(t)) \tag{8}$$

$$x_{i,d}(t+1) = x_{i,d}(t) + v_{i,d}(t+1) \tag{9}$$

Here, c_1 and c_2 denote the cognitive and social coefficients, while r_1 and r_2 are random factors ranging between 0 and 1. The terms $v_{(i,d)}(t)$ and $x_(i,d)(t)$ refer to the velocity and position of particle i within dimension d. The variables pbest and gbest correspond to the best position currently found by the individual particle and the best position identified across the entire swarm, respectively. The parameter ω, known as the inertia weight, acts as a convergence control factor. The flowchart of the PSO algorithm is depicted in Fig. 6.

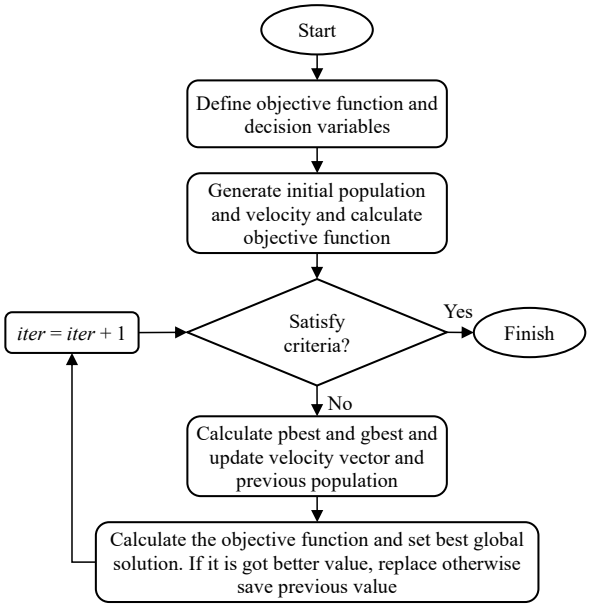

Fig. 6. Flowchart of the proposed controller parameters tuning based on PSO.

Table 1. The network parameters.

Parameter	Value	Parameter	Value
Resistance of nonlinear load	30Ω	Network voltage	220V
Capacitance of nonlinear load	$2200\mu F$	Frequency	50Hz
Resistance of linear load	30Ω	DC voltage	650V
Capacitance of LC filter	$27\mu F$	Switching frequency	9KHz
Resistance of LC filter	0.1Ω	Inductance of LC filter	0.7mH

Table 2. The parameters.

Symbol	Value	Symbol	Value
k	2	k_p	1.8
a_0	0.92	k_i	112.3
a_1	0.04	k_r	2.2

4. SIMULATION STUDY

The outcomes detailed in this section were derived from simulations using MATLAB software performed on a workstation featuring an 8-core processor operating at 3.5 GHz, 8 GB of RAM, a 12 MB cache, and a 1 TB internal storage drive. To evaluate the proposed control scheme for enhancing electrical power quality, the performance of the controller under different network conditions and load types has been investigated. For this purpose, a simple network consisting of an inverter connected to the power grid was considered. Three different case studies were conducted for simulation. In order to compare with the PI controller, the simulation was performed once without the proposed controller and again with the proposed controller, and the performance of the proposed controller was validated. The required values for the simulation, corresponding to the network (see Fig. 1) and the controller, are given in Table 1.

To solve the problem of optimal determination of control parameters by the algorithm, a population of 50 particles has been selected. To terminate the algorithm, the maximum number of iterations was set to 100. Also, the values of c_1 and c_2 were set to 2. The output values of the optimization algorithm, according to the proposed objective function, are given in Table 2.

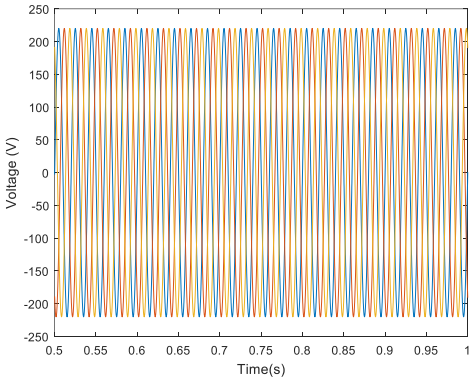

Fig. 7. Network voltage waveform – without non-linear loads and voltage distortion.

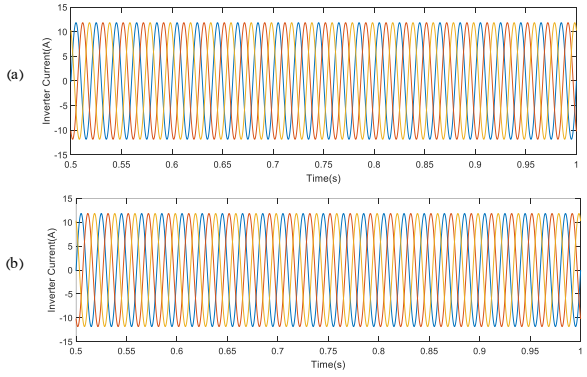

Fig. 8. Input current waveform to the network with controller – without non-linear loads and voltage distortion – (a): PI controller, (b) Proposed PI+RC controller.

- **Case study 1**

It is assumed that only one resistive (linear) load is connected in the local load of the inverter. The network has a sinusoidal voltage without distortion. The inverter must deliver a certain amount of power ($I_{od}^{ref} = 10A$) and ($I_{oq}^{ref} = 0A$) to the grid.

In this scenario, it is expected that due to the absence of any harmonic sources, the controllers will perform optimally. To compare the performance of the PI controller and the proposed PI+RC controller, the output results for the voltage at the Point of PCC, the inverter currents, the input current to the power network, the load current, the active and reactive power generated by the inverter, and the harmonic spectrum of the input current to the power network are shown in Figs. 7- 13, respectively.

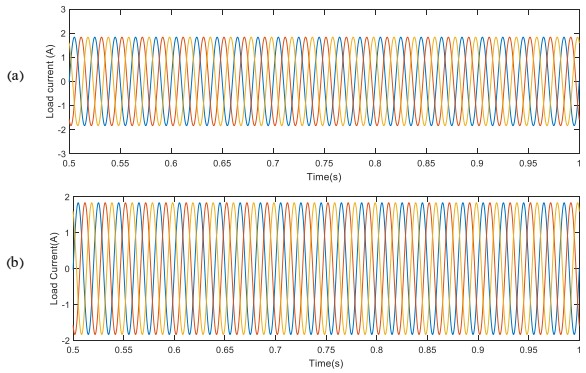

Fig. 9. Output current waveform of the inverter – without non-linear loads and voltage distortion – (a): PI controller, (b) Proposed PI+RC controller.

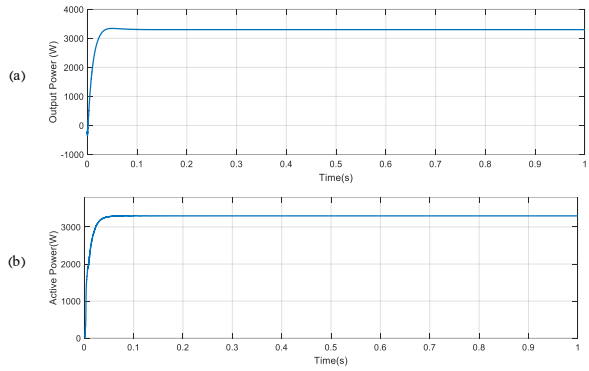

Fig. 10. Load current waveform without non-linear loads and voltage distortion – (a): PI controller, (b) Proposed PI+RC controller.

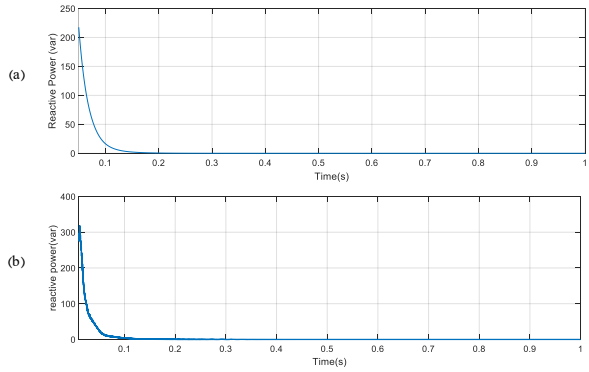

Fig. 11. Active power – without non-linear loads and voltage distortion – (a): PI controller, (b) Proposed PI+RC controller.

As there are no harmonic-producing sources or non-linear loads in this scenario, both the PI controller and the proposed PI+RC controller demonstrate similar performance, such that for both controllers, the THD of the input current to the power network is below one percent.

- **Case study 2**

In addition to the linear load, a non-linear load based on a diode rectifier is also connected to the local load. Due to the

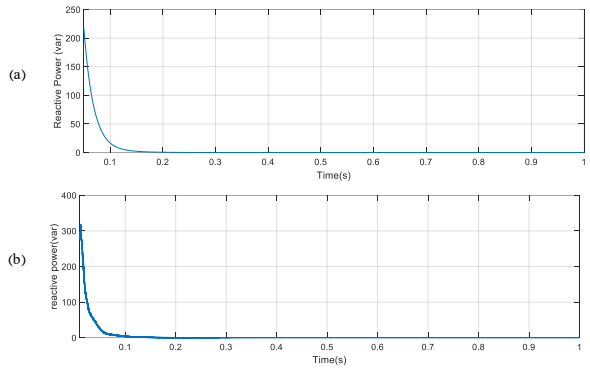

Fig. 12. Reactive power – without non-linear loads and voltage distortion – (a): PI controller, (b) Proposed PI+RC controller.

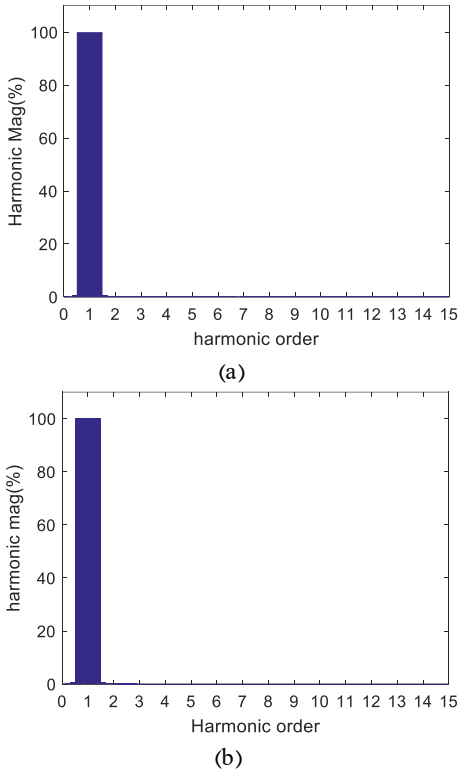

Fig. 13. Harmonic spectrum of the output current – without non-linear loads and voltage distortion – (a): PI controller, (b) Proposed PI+RC controller.

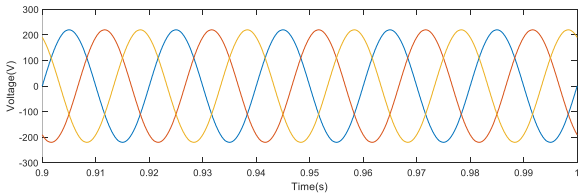

Fig. 14. PCC voltage waveform with the presence of non-linear load.

presence of the non-linear load, harmonic current is produced and enters the network. Similar to the previous case, the inverter must work in such a way that it not only delivers the specified power ($I_{od}^{ref} = 10A$) and ($I_{oq}^{ref} = 0A$) to the power grid, but also is able to bring the current THD to a standard level. In this scenario, due to the presence of a non-linear load (diode rectifier load), the load

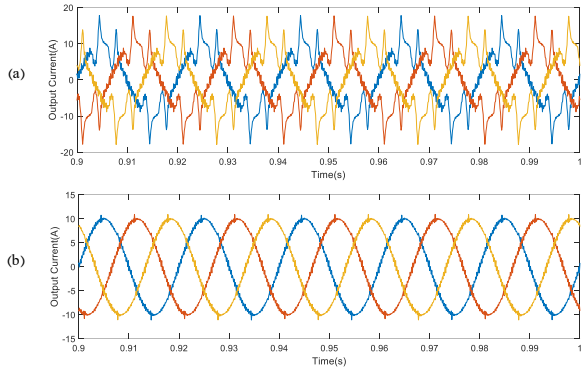

Fig. 15. Output current waveform with non-linear load – (a): PI controller, (b) Proposed PI+RC controller.

current and consequently, the inverter current and the input current to the power network have high harmonic content. In this case, the controllers should act in a way that achieves the control objective, which is to reduce the THD of the input current to the power network to the standard level of 5%.

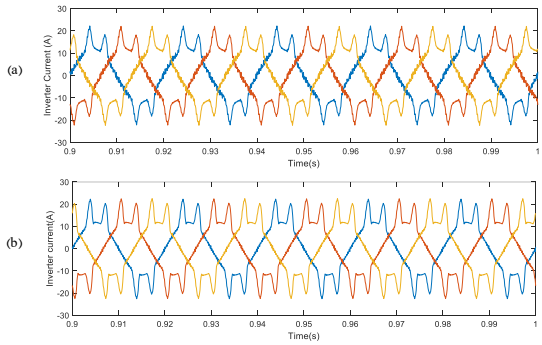

Fig. 16. Inverter current waveform with non-linear load – (a): PI controller, (b) Proposed PI+RC controller.

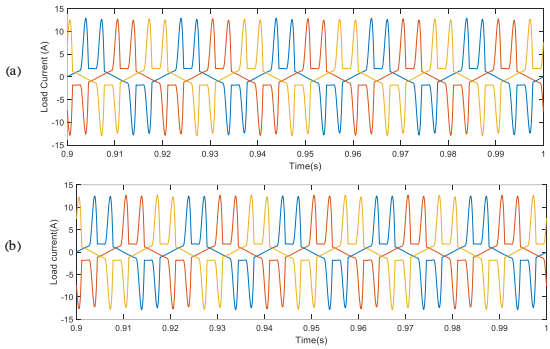

Fig. 17. Load current waveform with non-linear load – (a): PI controller, (b) Proposed PI+RC controller.

To compare the performance of the PI controller and the proposed PI+RC controller, the output results for the voltage at the Point of Common Coupling (PCC), the inverter currents, the input current to the power network, the load current, the active and reactive power generated by the inverter, and the harmonic spectrum of the input current to the power network are shown in Figs. 14– 20, respectively.

In this case study, non-linear loads cause the generation of harmonic currents. As depicted in Fig. 17, due to the presence of non-linear loads, the load current has a very high harmonic

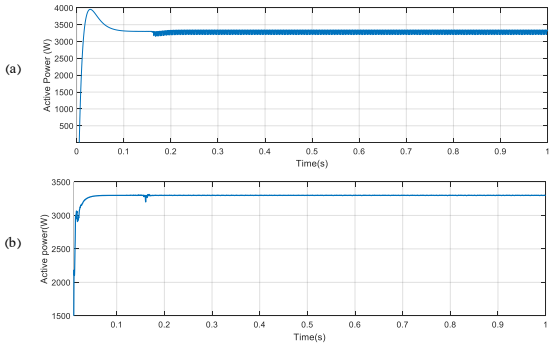

Fig. 18. Active power with non-linear load – (a): PI controller, (b) Proposed PI+RC controller.

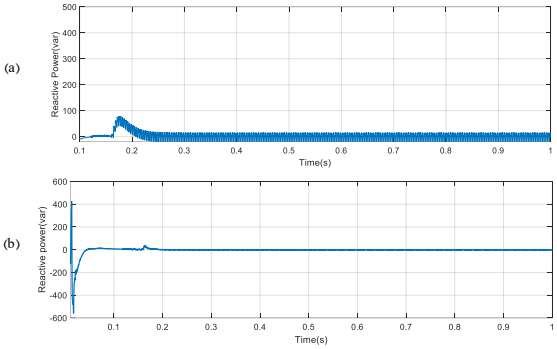

Fig. 19. Reactive power with non-linear load – (a): PI controller, (b) Proposed PI+RC controller.

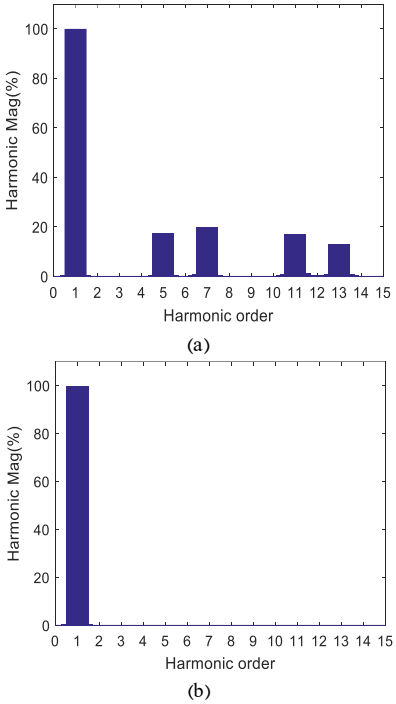

Fig. 20. Harmonic spectrum of output current with non-linear load – (a): PI controller, (b) Proposed PI+RC controller.

content. This harmonic load current enters the inverter and the power network, causing both the inverter current (Fig. 16-(a)) and the input current to the power network (Fig. 15-(a)) to contain harmonics. These results indicate that the PI controller did not

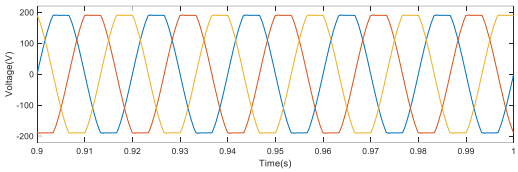

Fig. 21. Voltage waveform at PCC with non-linear load and network voltage distortion.

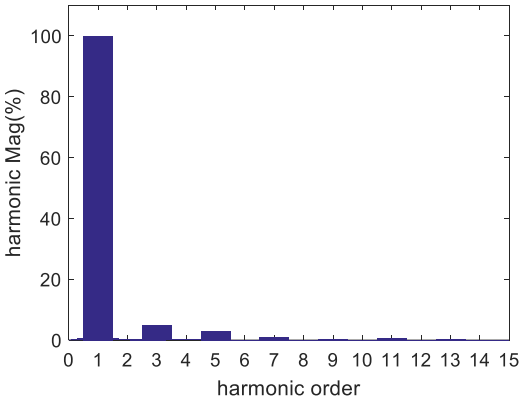

Fig. 22. Harmonic spectrum of network voltage at PCC with non-linear load and voltage distortion.

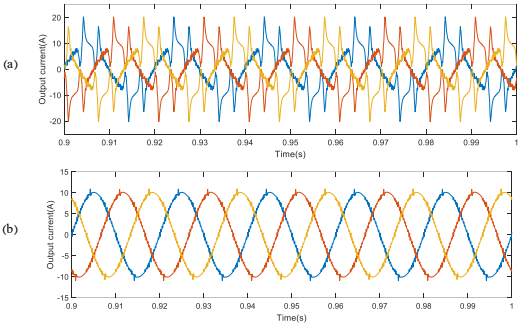

Fig. 23. Output current waveform with non-linear load and voltage distortion – (a): PI controller, (b) Proposed PI+RC controller.

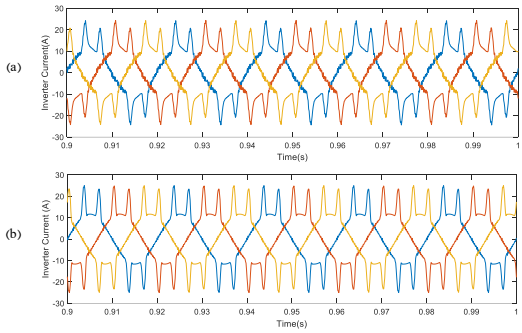

Fig. 24. Inverter current waveform with non-linear load and voltage distortion – (a): PI controller, (b) Proposed PI+RC controller.

perform well, with the THD of the input current to the power network being around 37.5%, which is very high. Additionally, the active and reactive power output of the inverter exhibit very high fluctuations.

However, with the implementation of the proposed PI+RC controller, although the load current still shows harmonics as seen

in Fig. 17, the input current to the power network, as shown in Fig. 16-(b), has become largely sinusoidal, and its harmonic content has been significantly reduced. As shown in Fig. 20-(a), the harmonic spectrum of the input current to the power network with the PI controller has other harmonics in addition to the main power frequency component, whereas Fig. 20-(b) shows that the input current to the power network only contains the main power frequency component. With the use of the proposed PI+RC controller, the THD of the input current to the power network has been reduced by 32 percentage points, from 37.5% to 5.6%. Additionally, the active and reactive power show very low fluctuation amplitudes. These results demonstrate the very effective performance of the proposed PI+RC controller.

- **Case study 3**

In addition to the presence of linear and non-linear load that leads to the generation of current harmonics, the network voltage at the PCC point also has distortion, which greatly increases the percentage of harmonic distortion. In addition to generating specified power ($I_{od}^{ref} = 10A$) and ($I_{oq}^{ref} = 0A$) and injecting it into the power grid, the controller must bring current THD to the standard level. Similarly, in this scenario, the load current, and consequently the inverter current and the input current to the power network, have a high harmonic spectrum. In this situation, the controllers must act in such a way that the control objective, which is to reduce the THD of the input current to the power network, is achieved at the standard level of 5%. To compare the performance of the PI controller and the proposed PI+RC controller, the output results for the voltage at the PCC, the inverter currents, the input current to the power network, the load current, the active and reactive power generated by the inverter, and the harmonic spectrum of the input current to the power network are shown in Figs. 21– 28, respectively.

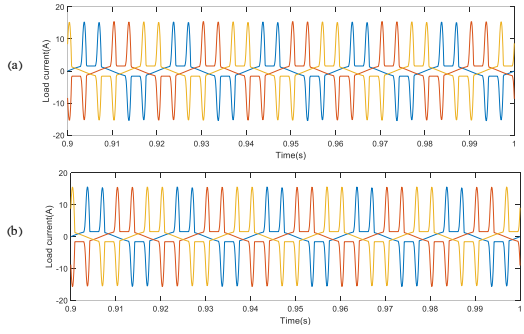

Fig. 25. Load current waveform with non-linear load and voltage distortion – (a): PI controller, (b) Proposed PI+RC controller.

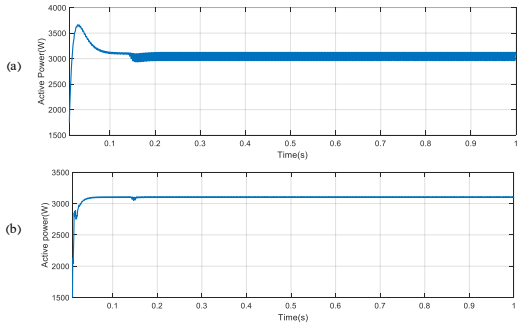

Fig. 26. Active power with non-linear load and voltage distortion – (a): PI controller, (b) Proposed PI+RC controller.

In this case study, non-linear loads cause the generation of harmonic currents. As depicted in Fig. 25, due to the presence of non-linear loads and distortion in the voltage at the PCC, the load current has a very high harmonic content. This harmonic load current enters the inverter and the power network, causing both the inverter current (Fig. 24-(a)) and the input current to the power network (Fig. 23-(a)) to become harmonic. These results show that the PI controller did not perform well, with the THD of the input current to the power network being around 49.5 percent, which is very high. Additionally, the active and reactive power output of the inverter has very high fluctuations.

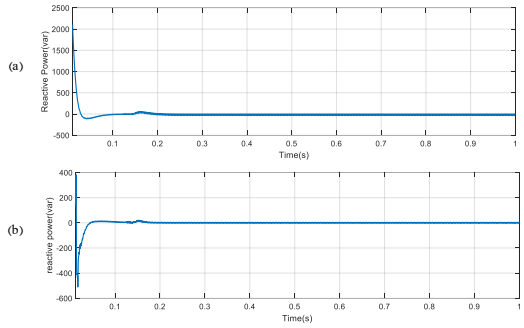

Fig. 27. Reactive power with non-linear load and voltage distortion – (a): PI controller, (b) Proposed PI+RC controller.

However, with the implementation of the proposed PI+RC controller, although the load current still shows harmonics as seen in Fig. 25, the input current to the power network, as shown in Fig. 23-(b), has become largely sinusoidal, and its harmonic content has been significantly reduced. According to Fig. 28-(a), the harmonic spectrum of the input current to the power network with the PI controller includes other harmonics in addition to the main power frequency component, whereas Fig. 28-(b) shows that the input current to the power network only has the main power frequency component. With the use of the proposed PI+RC controller, the THD of the input current to the power network has been reduced by 44 percent to 5 percent. Additionally, the active and reactive power has very low fluctuation amplitudes. These results demonstrate the very suitable performance of the proposed PI+RC controller.

Table 3. Comparison of THD for output current.

Case study no.	Output current THD (%) PI controller	PI+RC controller
1	3.5	3.2
2	37.3	5
3	49.5	5

To compare both controller behavior, the results from Table 3 can be used. It is observed that the proposed controller has a very suitable performance in eliminating harmonics and improving the quality of electrical power.

4.1. Discussion

The comparative evaluation of the two scenarios demonstrates the effectiveness and necessity of incorporating the Repetitive Controller (RC) into the traditional PI control scheme, particularly in environments characterized by harmonic distortions. In case study 1, where the system operates with a purely linear load and a distortion-free sinusoidal voltage source, both the PI controller and the proposed PI+RC structure exhibit nearly identical performance. As evidenced in Figs. 7 to 13, the waveforms of the network voltage, inverter current, load current, and the active/reactive power remain stable, with minimal harmonic distortion. The THD of the input current to the grid remains below 1% in both cases. This outcome confirms that under ideal conditions with negligible harmonic content, the PI controller alone is sufficiently capable

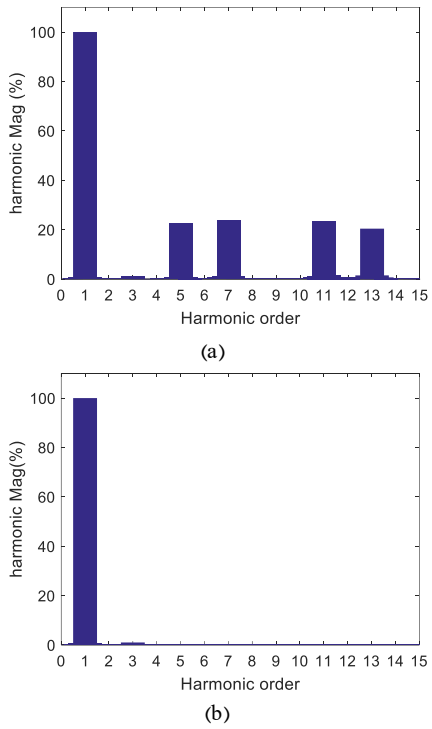

Fig. 28. Harmonic spectrum of output current with non-linear load and voltage distortion – (a): PI controller, (b) Proposed PI+RC controller.

of regulating power delivery and maintaining power quality. Since the harmonic content is inherently low, the RC's filtering function is not activated significantly, leading to similar results with or without its presence. In contrast, case study 2 introduces a more realistic and challenging scenario by including a nonlinear load (a diode rectifier). This setup introduces considerable harmonic distortion into the system. In such a condition, the standard PI controller falls short in mitigating the harmonic effects, as it lacks the inherent structure to selectively suppress harmonic components. This limitation is reflected in increased THD values in the input current to the grid, along with visibly distorted waveforms for both inverter and load currents. However, the introduction of the RC controller alongside the PI controller in the proposed scheme leads to a substantial improvement in harmonic suppression. The RC, designed to specifically target and attenuate periodic disturbances at selected harmonic frequencies (as highlighted by its high gain response at 6th, 12th, and higher-order harmonics), effectively filters out these components. As a result, the current injected into the grid exhibits a much smoother waveform, and the THD is significantly reduced compared to the standard PI controller alone. The proposed structure ensures that the reference signal used for switching is optimized to counteract the specific harmonic components, achieving the dual goals of power injection and power quality enhancement. The necessity for this enhancement becomes particularly evident in systems where nonlinear loads are prevalent a common condition in modern distributed generation systems and smart grid applications. Thus, while the additional complexity introduced by the RC controller may appear redundant in ideal conditions (as seen in case study 1), its contribution becomes crucial in realistic scenarios where harmonic disturbances cannot be ignored. In summary, the results across the two scenarios underscore the adaptive advantage of the proposed PI+RC control strategy. While maintaining baseline performance under ideal conditions, it delivers marked improvements in power quality under distorted conditions, justifying its implementation for robust harmonic mitigation in grid-connected inverter systems.

5. Conclusion

Inverters have the capability to convert direct voltage into alternating voltage and can be utilized either while connected to a network or in an isolated mode. Typically, when connected to the network, inverters operate in current control mode to deliver a specific and predetermined current at their output. Ideally, voltages and currents should be sinusoidal, but in reality, they contain distortion and harmonics. Nonlinear loads or distortions in the voltage source usually cause the voltages and currents in the network to become non-sinusoidal, leading to a reduction in the quality of electrical power. To improve the quality of electrical power, a control system has been designed and implemented for network-connected inverters to significantly reduce the injection of harmonics and distortion from the inverter to the network. The proposed controller is based on a proportional-integral controller within a synchronous rotating frame along with a repetitive control compensator. To evaluate the performance of the proposed controller, the controller has been applied to an inverter connected to the network that has a mixed local load of linear and nonlinear elements, and several case studies have been simulated. The results of the simulation demonstrate the effective performance of the proposed controller in reducing the amount of harmonic distortion injected into the network. In scenarios where nonlinear loads are present in the network or even when the power network voltage is distorted, the proposed PI+RC controller exhibits much lower THD compared to the PI controller alone. With just the presence of nonlinear loads, the THD of the output current has been reduced from 37.5% to 5.5%. Even in the presence of nonlinear loads and voltage distortion in the network, the THD has been reduced from 49.5% with the PI controller to 5% with the proposed controller. Additionally, the output of active and reactive power using the PI controller in the presence of harmonic distortion has high amplitude fluctuations, while these fluctuations are significantly reduced with the proposed method.

References

[1] K. Alijanzadeh and A. Ghasemi-Marzbali, "Optimal load distribution based on decision theory with information gap in the presence of wind farms connected to the power system," *J. Oper. Autom. Power Eng.*, 2024.

[2] A. Hussain and H. M. Kim, "A rule-based modular energy management system for ac/dc hybrid microgrids," *Sustainability*, vol. 17, no. 3, p. 867, 2025.

[3] M. Shadnam Zarbil and A. Vahedi, "Power quality of electric vehicle charging stations and optimal placement in the distribution network," *J. Oper. Autom. Power Eng.*, vol. 11, no. 3, pp. 193–202, 2023.

[4] M. B. Saïd-Romdhane, M. Haddad, and I. Slama-Belkhodja, "Innovative adaptive virtual impedance for resonance frequency mitigation in grid-connected converters," *Electr. Power Syst. Res.*, vol. 239, p. 111207, 2025.

[5] M. Aslan, B. Afif, M. Salmi, B. Merabet, M. Berka, and S. Masoud, "Performance enhancement of microgrid systems using backstepping control for grid side converter and mppt optimization," *Sol. Energy Sustain. Dev. J.*, vol. 14, no. 1, pp. 19–41, 2025.

[6] A. Seifi, S. H. Hosseini, M. Tarafdar Hagh, and M. Hosseinpour, "Capacitor based topology of cross-square-switched t-type multi-level inverter," *Sci. Rep.*, vol. 14, no. 1, p. 3166, 2024.

[7] H. Mansourizadeh, M. Hosseinpour, A. Seifi, and M. Shahparasti, "A 13-level switched-capacitor-based multilevel inverter with reduced components and inrush current limitation," *Sci. Rep.*, vol. 15, no. 1, p. 290, 2025.

[8] R. Ghanizadeh, M. Ebadian, and G. B. Gharehpetian, "Control of inverter-interfaced distributed generation units for voltage and current harmonics compensation in grid-connected microgrids," *J. Oper. Autom. Power Eng.*, vol. 4, no. 1, pp. 66–82, 2016.

[9] A. T. Alahmad, A. Saffarian, S. G. Seifossadat, and S. S. Mortazavi, "Frequency and voltage stability of the islanded microgrid with multi dc-bus based-inverter using droop control," *J. Oper. Autom. Power Eng.*, vol. 13, no. 2, pp. 121–126, 2025.

[10] N. R. Abjadi, "Nonsingular terminal sliding mode control for islanded inverter-based microgrids," *J. Oper. Autom. Power Eng.*, vol. 12, no. 1, pp. 26–34, 2024.

[11] K. Matharani and H. Jariwala, "Stability analysis of microgrid with passive, active, and dynamic load," *J. Oper. Autom. Power Eng.*, vol. 11, no. 4, pp. 295–306, 2023.

[12] M. R. Babaei, A. Ghasemi-Marzbali, and S. Abbasalizadeh, "Control of a combined battery/supercapacitor storage system for dc microgrid application," *J. Energy Storage*, vol. 96, p. 112675, 2024.

[13] H. S. Khan and A. Y. Memon, "Active and reactive power control of the voltage source inverter in an ac microgrid," *Sustainability*, vol. 15, no. 2, p. 1621, 2023.

[14] C. Sunil Kumar, C. Puttamadappa, and Y. L. Chandrashekar, "Power quality improvement in grid integrated pv systems with soa optimized active and reactive power control," *J. Electr. Eng. Technol.*, vol. 18, no. 2, pp. 735–750, 2023.

[15] T. Pidikiti, B. Gireesha, M. Subbarao, and V. M. Krishna, "Design and control of takagi-sugeno-kang fuzzy based inverter for power quality improvement in grid-tied pv systems," *Measurement: Sensors*, vol. 25, p. 100638, 2023.

[16] N. Kanagaraj, M. Vijayakumar, M. Ramasamy, and O. Aldosari, "Energy management and power quality improvement of hybrid renewable energy generation system using coordinated control scheme," *IEEE Access*, vol. 11, pp. 93254–93267, 2023.

[17] M. N. Tasnim, T. Ahmed, M. A. Dorothi, S. Ahmad, G. M. Shafiullah, S. M. Ferdous, and S. Mekhilef, "Voltage-oriented control-based three-phase, three-leg bidirectional ac–dc converter with improved power quality for microgrids," *Energies*, vol. 16, no. 17, p. 6188, 2023.

[18] S. K. Das, S. C. Swain, R. Dash, J. Reddy, C. Dhanamjayalu, R. Chinthaginjala, and A. ELrashidi, "Design and analysis of upqc in a microgrid using model reference adaptive control ensemble with back-stepping controller," *Heliyon*, vol. 10, no. 14, 2024.

[19] Y. Singh, B. Singh, and S. Mishra, "Control strategy for multiple residential solar pv system in distribution network with improved power quality," *IEEE Trans. Ind. Appl.*, vol. 59, no. 3, pp. 3686–3699, 2023.

[20] S. Choudhury and G. K. Sahoo, "A critical analysis of different power quality improvement techniques in microgrid," *e-Prime - Adv. Electr. Eng. Electron. Energy*, p. 100520, 2024.

[21] C. S. Goli, M. Manjrekar, P. Sahu, A. Chanda, and S. Essakiappan, "Implementation of stationary and synchronous frame current regulators for grid tied inverter using typhoon hardware-in-the-loop system," in *Proc. IEEE Int. Symp. Power Electron. Distrib. Gener. Syst.*, pp. 1–8, Jun. 2021.

[22] S. Golestan, J. M. Guerrero, and J. C. Vasquez, "Three-phase plls: A review of recent advances," *IEEE Trans. Power Electron.*, vol. 32, no. 3, pp. 1894–1907, 2017.

[23] H. Shayeghi and A. Younesi, "Mini/micro-grid adaptive voltage and frequency stability enhancement," *J. Oper. Autom. Power Eng.*, vol. 7, no. 1, pp. 107–118, 2019.

[24] Y. Li, J. Song, B. Duan, X. Li, and C. Zhang, "Repetitive control for harmonic compensation in three-phase isolated matrix rectifier," in *Proc. IEEE Ind. Electron. Soc. Annu. Conf.*, pp. 1443–1448, Oct. 2020.

[25] O. Abedinia, A. Ghasemi, and N. Ojaroudi, "Improved time-varying inertia weight pso for solving economic load dispatch with subsidies and wind power effects," *Complexity*, vol. 21, no. 4, pp. 40–49, 2016.